Si δ-doping of ⟨011⟩-oriented GaAs and $Al_xGa_{1-x}As$ grown by molecular-beam epitaxy

E. F. Schubert, Loren Pfeiffer, K. W. West, H. S. Luftman, and G. J. Zydzik
AT&T Bell Laboratories, 600 Mountain Avenue, Murray Hill, New Jersey 07974

(Received 18 November 1993; accepted for publication 31 January 1994)

Silicon δ-doping is studied on ⟨011⟩-oriented GaAs and $Al_xGa_{1-x}As$ grown by molecular-beam epitaxy. Hall measurements and secondary ion mass spectrometry on as-grown and on annealed samples reveal (i) that the electrical activity is reduced for the ⟨011⟩-oriented samples as compared ⟨001⟩-oriented reference samples, (ii) that the electron mobility is lower for ⟨011⟩-oriented samples, and (iii) that the thermal redistribution of Si impurities is comparable for both orientations. We find a markedly different dependence of the electron mobility on the spacer thickness in selectively doped ⟨011⟩-oriented $Al_xGa_{1-x}As$/GaAs heterostructures, which is explained by the reduced doping efficiency of Si in ⟨011⟩-oriented $Al_xGa_{1-x}As$.

The growth and doping of III-V semiconductors oriented off the ⟨001⟩ crystal axis is required for many advanced semiconductor structures including quantum wire structures grown on cleaved edges,[1] and for structures grown on nonplanar, patterned surfaces.[2] The doping properties on different surfaces may not be the same despite the cubic symmetry of the zincblende structure. Difficulties with doping and growth of ⟨011⟩ GaAs by molecular-beam epitaxy (MBE) have been reported,[3–5] and initial studies on Si doping of ⟨011⟩ GaAs by MBE have revealed highly resistive materials.[6,7] Si doping in ⟨011⟩ GaAs grown by organometallic vapor phase epitaxy (OMVPE) resulted in anomalous doping properties.[8–10] In the present study, we investigate Si doping properties in ⟨011⟩-oriented GaAs and $Al_xGa_{1-x}As$ and show that these properties can explain doping effects observed in ⟨011⟩-oriented $Al_xGa_{1-x}As$/GaAs heterostructures.

The epitaxial layers were grown by molecular-beam epitaxy on ⟨001⟩ and ⟨011⟩ GaAs substrates which were mounted side by side with Ga solder on a Ta substrate holder. The layers consist of 0.5-μm epitaxial GaAs containing a Si δ-doped sheet located 1000 Å below the surface. The growth of the $Al_xGa_{1-x}As$ heterostructures has been described previously.[1] A beam-equivalent As_4 ion gauge pressure of 1.6×10^{-5} Torr was determined at the substrate position. The Ga flux was adjusted to yield a growth rate of 0.5 ML/s which is equivalent to 1.473 Å/s. A growth temperature of 505 °C routinely yields a smooth and featureless morphology free of excess Ga. The samples were characterized by van der Pauw measurements and by secondary ion mass spectrometry (SIMS).

The Hall carrier concentrations of ten different samples are shown in Fig. 1 as a function of the nominal Si doping density. Five of the epitaxial layers were grown side by side on ⟨011⟩-oriented substrates and on ⟨001⟩ substrates. Reevaporation of Si is not expected to be significant at the low substrate temperature of 505 °C. SIMS measurements revealed that the Si density is independent of the growth orientation at this growth temperature. The doping concentration was calibrated on GaAs ⟨001⟩ samples by Hall measurements assuming $n = N_{Si}$. The ⟨001⟩-oriented samples therefore follow the dashed line which represents unity doping efficiency. At high two-dimensional doping densities of $N_{Si} > 10^{13}$ cm^{-2}, the free-carrier concentration decreases for ⟨001⟩ GaAs, as has been observed previously for ⟨001⟩ GaAs.[11]

In marked contrast, the ⟨011⟩-oriented samples shown in Fig. 1 exhibit a much lower doping efficiency. Assuming $n/N_{Si} = 100\%$ for ⟨001⟩ GaAs, the doping efficiency, n/N_{Si}, is only 25%–60% for the ⟨011⟩-oriented samples. Furthermore, no saturation of the free-carrier concentration is observed at high doping concentrations for ⟨011⟩ samples in contrast to the ⟨001⟩ samples. The low doping efficiency in ⟨011⟩ GaAs can be due to either electrically inactive (neutral) Si impurities or due to autocompensation, i.e., negatively charged Si impurities on As sites. To clarify the charge state of the Si and origin of the low doping efficiency, we next discuss the electron mobility of the samples.

The room-temperature Hall mobility is shown in Fig. 2 for the two crystal orientations. The electron mobilities in Si-doped ⟨011⟩ GaAs are clearly lower than the electron mobilities in the ⟨001⟩ GaAs reference samples. For free-carrier

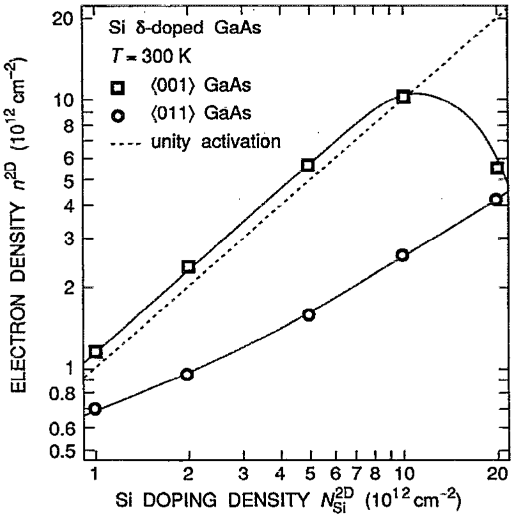

FIG. 1. Hall carrier concentration vs nominal Si doping density for ⟨011⟩ and ⟨001⟩ GaAs.

0003-6951/94/64(17)/2238/3/$6.00

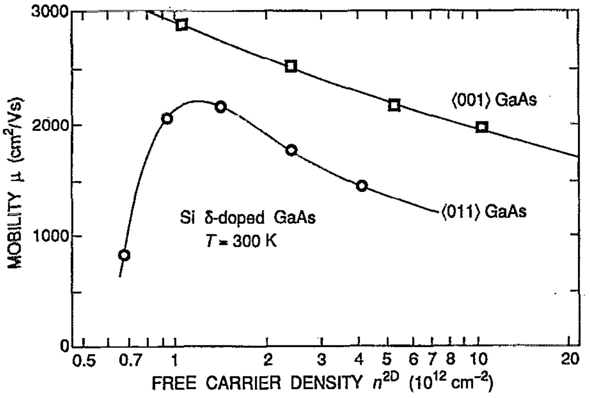

FIG. 2. Hall mobility as a function of the free-electron concentration for ⟨011⟩ and ⟨001⟩ GaAs at room temperature.

densities exceeding 1×10^{11} cm^{-2}, the values of the electron mobility are only two-thirds of the mobility values measured on ⟨001⟩ GaAs. The lower mobility indicates the presence of additional Coulombic scattering centers which are either Si acceptors, i.e., $\mathrm{Si_{As}}$, or positively charged Si complexes. We conclude that the lack of electrical activity in ⟨011⟩ GaAs *cannot* be due to inactive, neutral Si impurities, because the scattering caused by such neutral impurities is much weaker than scattering by ionized impurities.

We next examine the diffusion of Si in ⟨011⟩ GaAs during postgrowth annealing. The samples were heated to temperatures ranging from 600 to 950 °C in a rapid thermal annealer. Subsequently, the Si doping profiles were measured by secondary ion mass spectrometry. The SIMS profiles of the as-grown sample and of two samples annealed at 800 and 950 °C are shown in Fig. 3. All three samples have a peak concentration of 10^{19} cm^{-3} and a full width at half-maximum of 100 Å, which do not change significantly with annealing temperature. The profile width is resolution limited for the parameters used during the SIMS measurement. The results shown in Fig. 3 indicate that (i) no excessive redistribution of Si impurities occurs in ⟨011⟩ GaAs and that (ii) the redistribution of Si in δ-doped ⟨011⟩ Ga is not higher than the redistribution observed in Si-doped ⟨001⟩ GaAs.[12]

The study of Si in ⟨011⟩ $\mathrm{Al_{0.30}Ga_{0.70}As}$ by SIMS measurements provides evidence for a well-behaved distribution with no evidence for excessive diffusion during growth. Figure 4 shows the SIMS Si profile in a selectively doped $\mathrm{Al_{0.30}Ga_{0.70}As}$/GaAs heterostructure grown on a ⟨011⟩-oriented GaAs. The Si doping spike is in the $\mathrm{Al}_x\mathrm{Ga}_{1-x}\mathrm{As}$ 3500 Å below the $\mathrm{Al}_x\mathrm{Ga}_{1-x}\mathrm{As}$ surface and 400 Å above the semiconductor interface. The full width at half-maximum of the Si spike is 98 Å which is limited by the resolution of the SIMS instrument. We find that, as for ⟨011⟩ GaAs, the doping efficiency in ⟨011⟩ $\mathrm{Al}_x\mathrm{Ga}_{1-x}\mathrm{As}$ is lower than in ⟨001⟩ $\mathrm{Al}_x\mathrm{Ga}_{1-x}\mathrm{As}$. Thus an increase of the Si doping density by a factor of at least 2 is required of ⟨011⟩ heterostructures.[1]

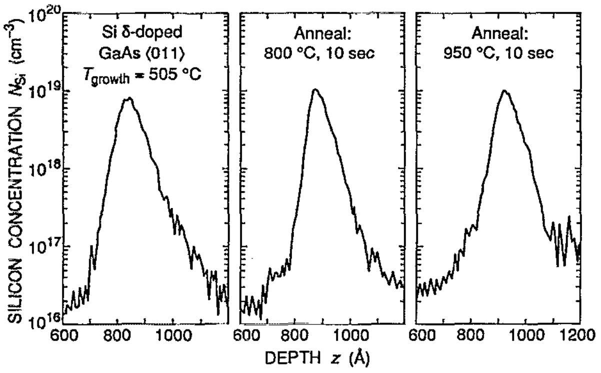

FIG. 3. Secondary ion mass spectrometry profiles of Si δ-doped ⟨011⟩ GaAs for an as-grown sample and after annealing at 800 and 950 °C for 10 s.

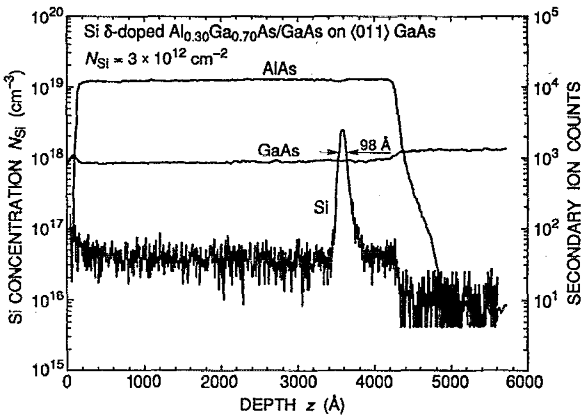

FIG. 4. SIMS profile of Si, AlAs, and GaAs of a selectively δ-doped $\mathrm{Al_{0.30}Ga_{0.70}As}$/GaAs heterostructure.

We next proceed to discuss a marked difference of the dependence of the electron mobility on the spacer thickness in ⟨001⟩ and ⟨011⟩ heterostructures. This dependence is shown for both orientations in Fig. 5. In both heterostructures, the electron mobility increases for large spacer thickness.[13] However, the mobility increases much more rapidly for the ⟨011⟩ orientation as compared to the ⟨001⟩ orientation. The stronger sensitivity of the ⟨011⟩ samples to the spacer thickness is explained as follows: For large spacer

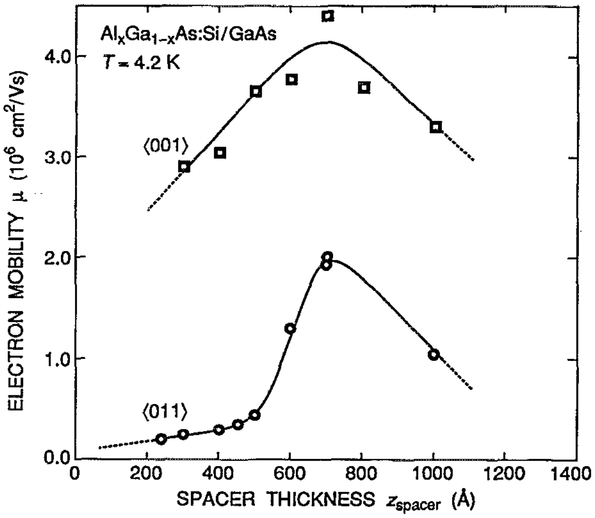

FIG. 5. Dependence of the electron mobility on the spacer width for heterostructures grown on ⟨011⟩- and ⟨001⟩-oriented GaAs substrates.

thicknesses, the mobility of ⟨001⟩ and ⟨011⟩ heterostructures is limited by scattering mechanisms *other* than remote ionized Si impurity scattering, for example, background impurity scattering, alloy scattering, phonon scattering, etc. As the spacer thickness decreases, remote ionized impurity scattering is becoming more important. For ⟨011⟩-oriented heterostructures, remote ionized impurity scattering will be stronger, due to the enhanced compensation discussed above. That is, since the doping efficiency n/N_{Si} is lower in ⟨011⟩ AlGaAs, the Si-doped layer contains more ionized impurities both positive and negative which rapidly reduce the electron mobility in the GaAs channel as the spacer thickness is decreased. This qualitative behavior is indeed displayed in Fig. 5.

In conclusion, we have studied Si δ-doped GaAs and $\mathrm{Al}_x\mathrm{Ga}_{1-x}\mathrm{As}$ grown on ⟨011⟩ GaAs by MBE and have compared the properties with epitaxial layers grown on ⟨001⟩ GaAs. We find that the electrical activity of Si in ⟨011⟩ GaAs is reduced to 25%–60% of its value in ⟨001⟩ GaAs. The mobility data suggest that the reduced activity is caused by negatively charged $\mathrm{Si}_{\mathrm{As}}^{-}$ or by negatively charged centers which include a Si impurity atom. The study of the diffusive redistribution of Si in ⟨011⟩ GaAs and ⟨011⟩ $\mathrm{Al}_x\mathrm{Ga}_{1-x}\mathrm{As}$ reveals minimal redistribution with no marked difference when compared to ⟨001⟩ GaAs. The dependence of the electron mobility on the spacer thickness of selectively doped heterostructures is much stronger for ⟨011⟩ heterostructures as compared to ⟨001⟩ heterostructures. This difference can be explained by the reduced electrical activity found in ⟨011⟩ material.

[1] L. Pfeiffer, K. W. West, H. L. Stormer, J. P. Eisenstein, K. W. Baldwin, D. Gershoni, and J. Spector, Appl. Phys. Lett. **56**, 1697 (1990).

[2] E. Kapon, in *Epitaxial Microstructures*, edited by A. C. Gossard (Academic, Boston, MA, 1993).

[3] W. I. Wang, J. Vac. Sci. Technol. B **1**, 630 (1983).

[4] L. T. P. Allen, E. R. Weber, J. Washburn, and Y. C. Pao, Appl. Phys. Lett. **51**, 670 (1987).

[5] J. Zhou, Y. Huang, Y. Li, and W. Y. Jia, J. Cryst. Growth **81**, 221 (1987).

[6] J. M. Ballingall and C. E. C. Wood, Appl. Phys. Lett. **41**, 947 (1982).

[7] J. M. Ballingall and C. E. C. Wood, J. Vac. Sci. Technol. B **1**, 162 (1983).

[8] X. Tang, E. P. Visser, P. M. A. van Lin, and L. J. Giling, J. Appl. Phys. **69**, 3278 (1991).

[9] X. Tang, J. te Nijenhuis, Y. Li, and L. J. Giling, J. Cryst. Growth **107**, 263 (1991).

[10] K. Okamoto, M. Fusuta, and K. Yamaguchi, Jpn. J. Appl. Phys. L **27**, 2121 (1988).

[11] E. F. Schubert, R. F. Kopf, J. M. Kuo, H. S. Luftman, and P. A. Garbinski, Appl. Phys. Lett. **57**, 497 (1990).

[12] E. F. Schubert, J. B. Stark, T. H. Chiu, and B. Tell, Appl. Phys. Lett. **52**, 293 (1988).

[13] E. F. Schubert, *Doping in III-V Semiconductors* (Cambridge University Press, Cambridge, 1993).